ISSN 0016-7029, Geochemistry International, 2023, Vol. 61, No. 11, pp. 1109–1127. © The Author(s), 2023. This article is an open access publication.
Russian Text © The Author(s), 2023, published in Geokhimiya, 2023, Vol. 68, No. 11, pp. 1113–1132.

Source and Generation Parameters of the Granitoid Melts of the Archean Charnockite–Enderbite Complex in Karelia, with Reference to the Pon'goma-Navolok Massif

V. M. Kozlovskii[a, b, *], E. B. Kurdyukov[a, **], M. A. Yakushik[a, c], V. V. Travin[d, e], T. F. Zinger[f], A. I. Yakushev[a], M. M. Fugzan[g], T. I. Kirnozova[g], and S. A. Ushakova[h]

[a] *Institute of Geology of Ore Deposits, Petrography, Mineralogy, and Geochemistry (IGEM), Russian Academy of Sciences, Moscow, 119017 Russia*

[b] *Ordzhonikidze Russian State University for Geological Exploration (MGRI), Moscow, 117997 Russia*

[c] *Korzhinskii Institute of Experimental Mineralogy (IEM), Russian Academy of Sciences, Chernogolovka, Moscow oblast, 142432 Russia*

[d] *Institute of Geology (IG), Karelian Research Center, Russian Academy of Sciences, Petrozavodsk, 185910 Russia*

[e] *Petrozavodsk State University, Petrozavodsk, 185910 Russia*

[f] *Institute of Precambrian Geology and Geochronology (IGGD), Russian Academy of Sciences, St. Petersburg, 199034 Russia*

[g] *Vernadsky Institute of Geochemistry and Analytical Chemistry (GEOKhI), Russian Academy of Sciences, Moscow, 119991 Russia*

[h] *Geological Faculty, Moscow State University, Moscow, 119991 Russia*

**e-mail: bazily.koz@gmail.com*

***e-mail: e-kurdukov@yandex.ru*

Received January 30, 2023; revised April 7, 2023; accepted April 14, 2023

Abstract—The paper presents authors' original detailed data on rocks of the Archean Pon'goma-Navolok charnockite–enderbite complex in northern Karelia. The rocks practically have not been modified and are preserved within a rigid block among Paleoproterozoic zones of ductile deformations and metamorphism. The geochemistry of the rocks and their isotope–geochemical features indicate that the protolith from which the enderbite melts of the main phase of the massif were derived may have been amphibolites. The enderbite melts were derived from these amphibolites under the effect of K_2O-, Na_2O-, and SiO_2-bearing fluids; and the enderbites were subsequently charnockitized with the involvement of fluids enriched in K_2O and SiO_2. Physicochemical modeling indicates that the enderbite melt was derived from the amphibolite protolith at a depth of about 45 km (P = 14.8 kbar, T = 1030–1080°C) under the effect of saline H_2O–CO_2 fluid. Comparison of the P–T parameters of the granulite-facies metamorphism of the metabasites and the parameters under which the enderbite melts were derived indicates that Archean granulite-facies metamorphism in the Belomorian belt in northern Karelia was of contact but not regional nature and was induced by the high-temperature field of an emplaced enderbite massif. The orthogneisses hosting the Pan'goma-Navolok massif inherit geochemical features of the unsheared, ungneissose, and unmetamorphosed enderbites. This means that enderbites analogous to those of the Pan'goma-Navolok massif may have served as the protolith of some of the orthogneisses, and that enderbites may have been spread more widely in the Archean than the currently preserved single enderbite massifs.

Keywords: granulite-facies metamorphism, enderbite, charnockite, amphibolite, Belomorian Mobile Belt

DOI: 10.1134/S0016702923090069

INTRODUCTION

Archean charnockite–enderbite complexes, which occur as massifs and domes in fields of high-temperature (to the granulite facies) metamorphism, are typical structural elements of Precambrian mobile belts. They have long been known and studied in much detail in the Belomorian–Lapland Mobile Belt in the Fennoscandian shield (Perchuk et al., 1999, 2006; Korol', 2005, 2018), in the Limpopo granulite belt between the Kaapvaal and Zimbabwe cratons in South Africa, in the Sharyzhalgai inlier of the basement of the Siberian craton (Petrova and Levitskii, 1984), and in many other ancient crystalline complexes. Data recovered by studying enderbite–charnockite compositions shed light onto many aspects of the evolution of the continental crust in the Precambrian. However, intense metamorphic processes related to Proterozoic and later tectonic reactivation of Archean cratons

often obliterate the primary high-temperature mineral assemblages. Metamorphism overprinted onto Paleoproterozoic deformation zones usually partly obliterates evidence of the magmatic nature of the charnockite–enderbite complexes. Because of this, studying charnockite–enderbite complexes that have preserved their primary mineral assemblages and geological relations between their Archean rocks, and which are very rare, is of paramount importance for understanding their nature.

The territory of the Belomorian Mobile Belt (hereafter BMB) in northern Karelia is known to host many Archean enderbite–charnockite complexes (Korol', 2005, 2018), but most of them contain very poorly preserved (if any and at all) mineral assemblages corresponding to the peak of their Archean granulite-facies metamorphism. These assemblages are fairly well preserved in the Pon'goma-Navolok massif in the Kem segment of BMB, 6 km southeast of the mouth of the Pon'goma River (Supplementary 1) and in the Karetskii massif in southern Belomorie. In this paper, we tried to shed light onto and resolve the following problems related to the nature of Archean charnockite–enderbite complexes in Belomorie, with reference to the Pon'goma-Navolok massif: (1) what was the probable source of the melts parental for the main-phase enderbites of the massif; (2) what were the physicochemical parameters under which these melts were generated; and (3) how these data correlate with the composition and metamorphic parameters of the host rocks.

GEOLOGY AND PETROGRAPHY OF THE PON'GOMA-NAVOLOK MASSIF

The Pon'goma-Navolok massif (which crops out over an approximate area of 1 × 2 km) was discovered by L.A. Kosoi, K.M. Koshits, and N.G. Sudovikov in the course of geological survey in 1935 (Kosoi, 1936; Sudovikov, 1937). The geological structure and petrology of the massif and the age of its rocks were discussed in numerous publications (Sudovikov, 1939; Shurkin, 1980; Zinger et al., 1993, 1994, 1999; Baikova, 2001, 2005; Drugova, 1977, 1996, 1997; Stenar' and Volodichev, 1970; Volodichev, 1975; Stepanov and Slabunov, 1994; Korol', 2009, 2011, 2018; Levchenkov et al., 1996; Levskii et al., 2009). Geological maps of this massif were published in (Sudovikov, 1937; Shurkin, 1980; Zinger et al., 1996; Stepanov and Slabunov, 1994), and the most detailed map of both the massif itself and its metamorphic surroundings was presented in (Kozlovskii et al., 2021; Supplementary 2) and was based on result of the 2017–2019 fieldwork carried out by V.M. Kozlovskii, V.V. Travin, and T.F. Zinger.

The Pon'goma-Navolok massif is a fragment of a rigid Archean block, which is bounded by Paleoproterozoic ductile shear zones (Ramsay and Huber, 1987) and high-pressure metamorphic rocks in the northwest and southeast (Supplementary 2). The rocks of the massif are only weakly sheared, contrary to what is typical of the Paleoproterozoic zones of high-pressure metamorphism. In most of the massif (except only its marginal portions adjacent to ductile deformation zones), the intrusive rocks preserve textures, mineral assemblages, and chemical composition of the Archean magmatic rocks.

The massif is made up of three phases. The main phase consists of orthopyroxene–clinopyroxene enderbites (*Pl* + *Cpx* + *Opx* + *Qtz* + *Ilm* ± *Amph* ± *Bt*). The most widely spread mesocratic enderbites host single lenses (0.2 × 0.5 m) of melanocratic enderbites that are slightly richer in mafic minerals and poorer in plagioclase. The leucocratic enderbites, which are richer in plagioclase, make up a suite of branching veins. The emplacement age of the orthopyroxene–clinopyroxene enderbites of the main phase (dated on the long-prismatic generation of zircon 1 with oscillatory zoning) is 2728 ± 21 Ma (Levchenkov et al., 1996). The later phase is dikes of northeastern and northwestern trend; these dikes consist of fine-grained and pegmatoid biotite-bearing charnockite and are 0.2–3 m thick and 10–30 m long. They are hosted mostly in the central part of the massif. Where charnockite dikes are abundant, the enderbites are metasomatized and recrystallized, with potassic feldspar rims developing between plagioclase grains, newly formed pyroxene replacing the magmatic clinopyroxene and orthopyroxene, biotite rims replacing orthopyroxene, and amphibole rims replacing mafic minerals. In the enderbites, this process was responsible for the origin of zircon II: roundish crystals with oscillatory zoning. The age of this zircon generation is 2728 ± 21 Ma (Levchenkov et al., 1996).

The third phase, which has been studied least comprehensively, is small (3–10 m) equant or vein-shaped bodies of equant and vein-shaped bodies of coarse-grained or pegmatoid biotite granite, which are found mostly in the eastern and central parts of the massif. These granites cut the first-phase enderbites, and their bodies in the enderbites are ubiquitously surrounded by K-feldspathization zones.

The eastern part of the massif hosts large tabular metabasite blocks 10–30 m thick and 50 to 800 m long. The blocks and the gneissosity of their rocks trend northwestward, conformably with the trends of the major structural elements of the complexes composing BMB. Some of the blocks are broken into lens-shaped fragments. The large sizes, little varying trends, and the absence of any indications of rotation suggest that these blocks cannot be typical xenoliths entrained by the melt from greater depths but that they are rather fragments of the walls and/or roof of the magma chamber, which were detached by the melt and sank in it, without any significant transport of these blocks along the magma channel.

The metabasites are Archean amphibolites (*Amph* + *Pl* + *Qtz*) that are no younger than 2.85 ± 0.01 Ga (Slabunov, 2008). These amphibolites were

overprinted by two younger metamorphic associations. One of them is the high-temperature (granulite-facies) assemblage (*Opx* + *Cpx* + *Pl* + *Qtz*), which was produced when the amphibolites were affected by the heat of the emplaced Archean enderbite intrusion, and the other is a high-pressure eclogite-like assemblage (*Grt* + *Cpx* + *Pl* + *Qtz*), produced when the metabasites were recycled when the Paleoproterozoic ductile flow zones were formed in the surroundings of the massif.

The metabasite blocks yield a prograde $P-T$ path from the amphibolite- to granulite-facies transformations. They started with the association of clinopyroxene amphibolites at temperatures of 690–760°C and pressures of 8.3–10.0 kbar, whereas the metamorphic culmination produced the clinopyroxene–orthopyroxene–plagioclase granulites at T = 830–910°C, P = 10.3–11.0 kbar (Kozlovskii et al., 2022). Granulite associations occur in the metabasites as domains, 1–5 mm across, of equigranular (hornfels) texture. The occurrence of this texture and some other features of the metabasites led G.M. Drugova (1996) to suggest, when she studied granulites in Tupaya Bay in the Chupa segment of BMB, that these rocks are of contact-metamorphic nature. It should be mentioned that neither the metamorphic rocks hosting the massif nor the metabasite blocks within this massif show evidence of granulite-facies metamorphism and migmatization[1]. The metabasite blocks also do not show evidence of any fluid influence of the enderbites.

The Pon'goma-Navolok massif is cut by garnet metagabbro dikes. This dike suite is well known in BMB and was emplaced into the Chupa segment at 2177 ± 11 Ma, whereas the age of the high-pressure metamorphism overprinted onto these dikes was dated at 1880–1890 Ma (Skublov et al., 2013). The high-pressure metamorphism formed and metabasite blocks a similar and highly specific patchy structure of these dikes, which is defined by large (up to 20–25 mm) equant glomerophyric aggregates of newly formed garnet and clinopyroxene, with the orthopyroxene replaced thereby by garnet[2]. The large garnet aggregates are grouped along some directions roughly parallel to the northeastern trend of the ductile flow zone in the central domain. In this case, the metabasites acquire a veinlet structure[3]. Thus the eclogite-like *Grt* + *Cpx* + *Pl* + *Qtz* association replaced both the Archean amphibolites and the Paleoproterozoic metagabbro dikes that cut across the massif. Moreover, the *Grt* + *Cpx* + *Pl* + *Qtz* eclogite-like rocks developing after the amphibolites are widespread in the outer metamorphic surroundings of the Pon'goma-Navolok massif and elsewhere in BMB, where these rocks are readily identified thanks to their specific patchy and veined structure. Hence, the *Grt* + *Cpx* + *Pl* + *Qtz* association was formed by regional Paleoproterozoic metamorphism. Traces of this metamorphism in the enderbites are discernible only in the gneissose marginal parts of the massif, where the enderbite assemblage *Opx* + *Cpx* + *Pl* + *Qtz* is overprinted by the assemblage *Bt* + *Grt* + *Pl* + *Qtz*, which is analogous to that of the orthogneisses in the metamorphic host rocks of the massif.

ANALYTICAL TECHNIQUES

Major components were analyzed by XRF at the Center for Collective Use of Analytical Equipment at IGEM RAS. The analysis was carried out on an Axios (PANalytical, Netherlands) vacuum spectrometer coupled to a 4-kW X-ray tube with an Rh anode. The maximum voltage of the tube was 60 kV, and the maximum anode current was 160 mA. The analysis was conducted according to the routine 439-RS NSAM VIMS 2010. Samples were prepared for their analysis by the technique of fusion with borates. The analytical errors corresponded to category-III accuracy of quantitative analysis according to OST RF 41-08-205-04. Regardless of the actual Fe oxidation state, all iron is represented in the form of $Fe_2O_{3\,tot}$.

Trace elements and REE were analyzed by ICP-MS at the Analytical Center of the Karelian Research Center, Russian Academy of Sciences, in Petrozavodsk, on a X-SERIES 2 (Thermo Fisher Scientific) quadrupole mass spectrometer, following the routine (Svetov et al., 2015). The powdered sample (100 mg) was decomposed by acids in an open system. The sensitivity of the tool throughout the whole mass scale was calibrated using standard reference 68-element (ICP-MS-68A-A) and 13-element (ICP-MS-68A-B) solutions by the High-Purity Standards Company, including calibrations for all of the analyzed elements. The quality of the analysis and the drift of the tool were controlled by alternating analyses of the samples and standards at a rate of 1 : 15 to 1 : 20. The standards were SGD-2A, S-1412, and BHVO-2, which were decomposed together with the set of analyzed samples. Most elements were analyzed accurate to 7 relative %, and Co, Ni, Y, and Ta were analyzed accurate to 7–12 relative %.

The isotope studies were carried out at the Laboratory of Isotope Geochemistry and Geochronology of Vernadsky Institute (GEOKhI). Concentrations of Rb, Sr, Sm, and Nd were analyzed by the isotope dilution (ID) technique (Kostitsyn and Zhuravlev, 1987): weighed amounts of solutions with mixed ^{87}Rb–^{84}Sr and ^{149}Sm–^{150}Nd tracers were added to the powdered

[1] The ortho- and clinopyroxene occasionally found by G.M. Drugova (1996) in Beluzh'ya Luda Island 7 km northwest of the Pon'goma-Navolok massif seem to be of relict nature.

[2] An unequilibrated character of garnet and clinopyroxene in there rocks was detected and described by G.M Drugova et al., (1977).

[3] The highly specific and locally occurring style of the Paleoproterozoic metamorphism overprinted onto the Archean metabasites makes it possible to separately sample these rocks during fieldwork. This is usually much harder to do in gneiss complexes.

samples, and the samples thus prepared were then decomposed with HNO_3 + HF mixture. First, the Rb, Sr, and an REE fraction was separated in columns with DowexW 50 × 8 ion exchanging resin by stepwise elution with 2.2 N HCl (for Rb) and 4.0 N HCl (for Sr and REE). Sm and Nd were extracted from the REE fraction in polyethylene columns with Ln-spec ion-exchanging resin, with stepwise elution with 0.15 N HCl, 0.3 N HCl, and 0.7 N HCl.

The Rb, Sr, Sm, and Nd isotope ratios were measured on a nine-collector Triton spectrometer in static mode. A correction for Sr isotope fractionation was introduced by normalizing the measured values to the ratio $^{86}Sr/^{88}Sr = 0.1194$. The normalized ratios were adjusted to $^{87}Sr/^{86}Sr = 0.71024$ in the internationally certified standard SRM-987. When the results were processed, the values were normalized: Nd isotopes to the $^{148}Nd/^{144}Nd$ ratio and those of Sm to $^{152}Sm/^{147}Sm$. The measurement methods are described in much detail in (Revyako et al., 2012). The average value of the Nd isotopic composition for the JNdi-1 standard (Tanaka et al., 2000) during our study was $^{143}Nd/^{144}Nd = 0.512114 \pm 6$ (2σ; $N = 10$). The blanks of the measured Sm/Nd ratio were assumed to be 0.1% of the values. The blanks during the experiment were 0.4 ng for Rb, 0.8 ng for Sr, 0.01 ng for Sm, and 0.001 ng for Nd. The measurements for the $^{147}Sm/^{144}Nd$ ratios were accurate to ±0.1%, and those for the $^{143}Nd/^{144}Nd$ ratio were accurate to ±0.005% (2σ).

The isochron plots were constructed and the age values were calculated with the ISOPLOT software (Ludwig, 2003). The εNd(t) values and initial $(^{87}Sr/^{86}Sr)_0$ ratios were calculated using the decay constants $\lambda^{87}Rb = 1.42 \times 10^{-11} \times year^{-1}$, $\lambda^{147}Sm = 6.54 \times 10^{-12} \times year^{-1}$ and the modern ratios of CHUR $^{143}Nd/^{144}Nd = 0.512638$, $^{147}Sm/^{144}Nd = 0.1967$ (Jacobsen and Wasserburg, 1984). The ratios of the depleted mantle $^{143}Nd/^{144}Nd = 0.513151$, $^{147}Sm/^{144}Nd = 0.21365$ were assumed according to (Goldstein and Jacobsen, 1988).

Tables of XRF and ICP-MS analyses of the rocks are presented in Supplementaries 3 and 4.

GEOCHEMISTRY OF THE ENDERBITES, CHARNOCKITES, BLOCKS OF METABASITES AND GNEISSES IN THE SURROUNDINGS OF THE PON'GOMA-NAVOLOK MASSIF

In the $Al_2O_3/(Na_2O + K_2O)$–$Al_2O_3/(CaO + Na_2O + K_2O)$ diagram (Frost et al., 2001), the enderbites and charnockites of the Pon'goma-Navolok massif plot within the field of I-type granites (Fig. 1b), which implies that their protolith was a magmatic rock (or rocks), likely mafic ones. The more calcic and less alkaline enderbites fall into the field of intermediate Al#, whereas the charnockites have higher Al#. As seen in the SiO_2–FeO/(FeO + MgO) diagram (Fig. 1a), the charnockites are notably richer in iron than the enderbites.

The amphibolites in blocks within the massif and compositionally similar amphibolites in its mafic surroundings occur in BMB as long domains, which are interpreted as Archean greenstone belts (Slabunov, 2008). Ratios of the logarithms of concentrations of trace elements (Mg–Fe, Ca–Fe, Mn–Fe, Zn–Fe, Ni–Fe, Sc–Fe, Ti–Fe, Co–Ni, Sr–Ba, Zr–Nb, Zn–Ti, Ti–V, P–Nb, and P–REE) in amphibolite in the blocks and in the enderbites (Fig. 2) indicate that the mesocratic enderbites of the main intrusive phase of the massif and the amphibolites plot on the same correlation lines. The enderbites are poorer in Fe, Mg, Mn, Ca, Ti, Ni, Co, Sc, Zn, and V than the amphibolites and richer in REE, Sr, Ba, Zr, Nb, and P.

The compositions of the enderbites and amphibolites correspond to the Rayleigh fractionation of these components in a closed system, which implies genetic relations between the rocks. The leucocratic and melanocratic enderbites sometimes plot away from the correlation lines for some elements. These deviations may have been caused by that the compositions of the rocks were altered by late magmatic and/or postmagmatic processes.

The behaviors of Si, Na, and K notably differ from those of other major cations. The enderbites are strongly enriched in Si, Na, and K relative to the amphibolites, and these elements do not define correlations for the enderbites–amphibolites. However, the rocks of the massif are leucocratic, mesocratic, and melanocratic enderbites that define obvious correlations, in which no amphibolites are involved. Si definitely strongly negatively correlates with Fe, Mg, Ca, Mn, Ti, and Na and positively with K. Therewith Na is weakly positively correlated with Al, and K is negatively correlated with Al (Figs. 3a–3i).

The two groups of the correlations likely suggest two processes that generated the rocks of the Pon'goma-Navolok massif. The earliest of the processes was the allochemical derivation of the enderbites from their hypothetical amphibolite protolith as a result of its interaction with metamorphic fluid enriched in K, Na, and SiO_2 compounds. The later process was the crystallization and differentiation of the enderbite melt in a magma chamber. Because the latter process was not related to the amphibolite protolith, the compositions of the amphibolites (solid squares in Fig. 3) do not plot onto the correlation lines. The earlier derivatives are the melanocratic enderbites. They are rich in mafic minerals and contain calcic plagioclase poor in the orthoclase component. The later derivatives are the leucocratic enderbites, and they contain less plagioclase and more potassic feldspar and quartz.

The likely source of material for the charnockites may have been the main-phase enderbites. Recall that the charnockite dikes are thin, always occur within the enderbite massif, and do not extend outside it. The

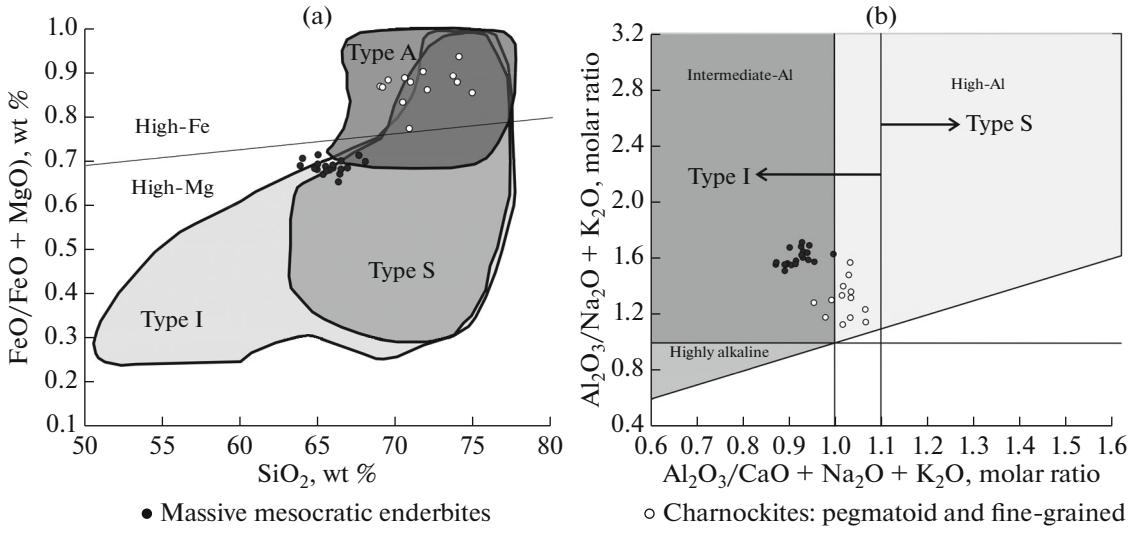

Fig. 1. Discriminant diagrams for granitoids (Frost et al., 2001) showing the composition of rocks of the Pon'goma-Navolok massif.

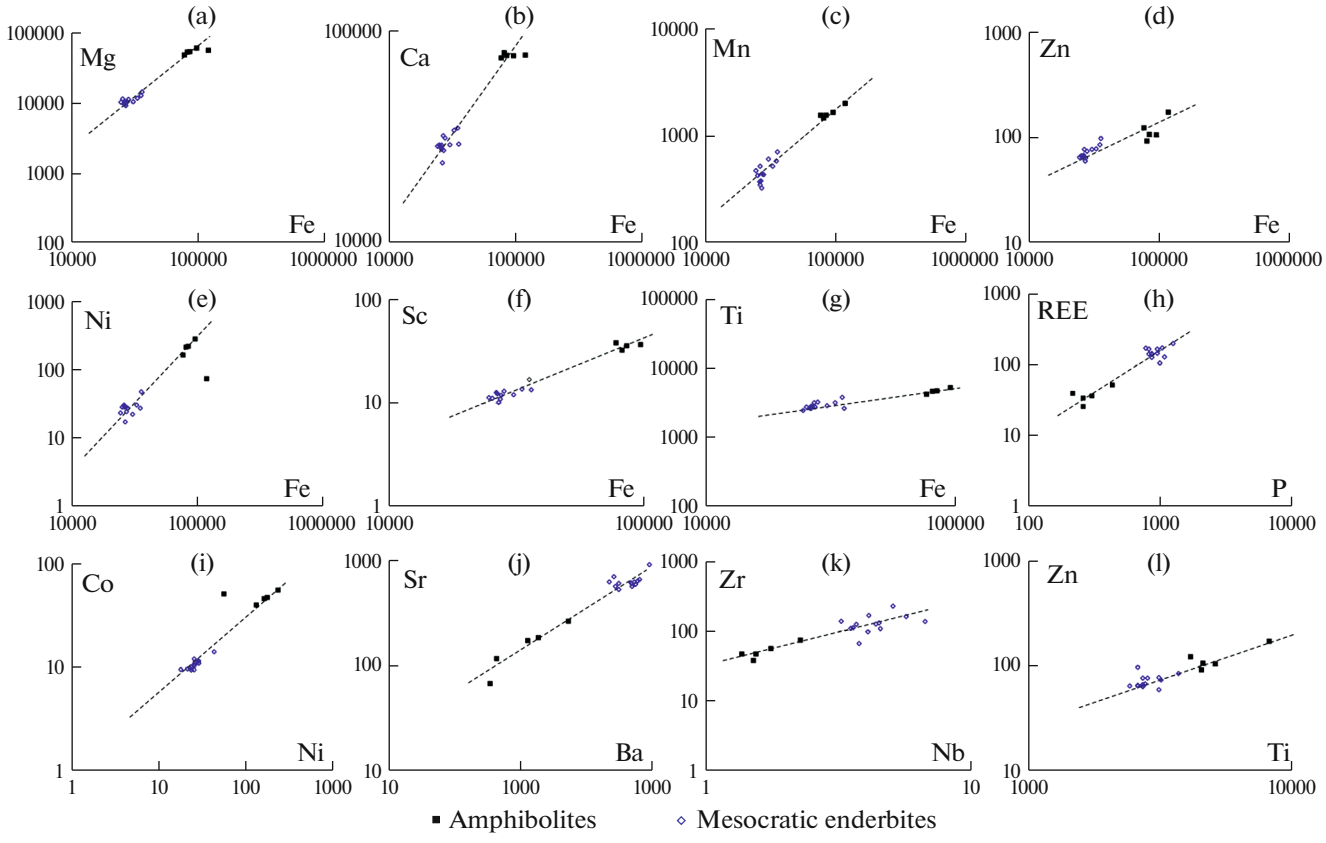

Fig. 2. Paired logarithmic ratios of major components and trace elements (ppm) in the amphibolites and enderbites of the Pon'goma-Navolok massif, illustrating their genetic relations. Dashed lines show correlations.

paired logarithmic ratios of incompatible elements, for example, Y–Nb, Ti–Nb, Ti–Y, Y–(total REE), Y–Yb, P–(total REE), and P–La of the enderbites and charnockites indicate that the compositions of these rocks plot very close to the correlation lines (Figs. 4a, 4b, 4c, 4d).

This indicates that the charnockites and enderbites may have evolved from the same source. The rocks

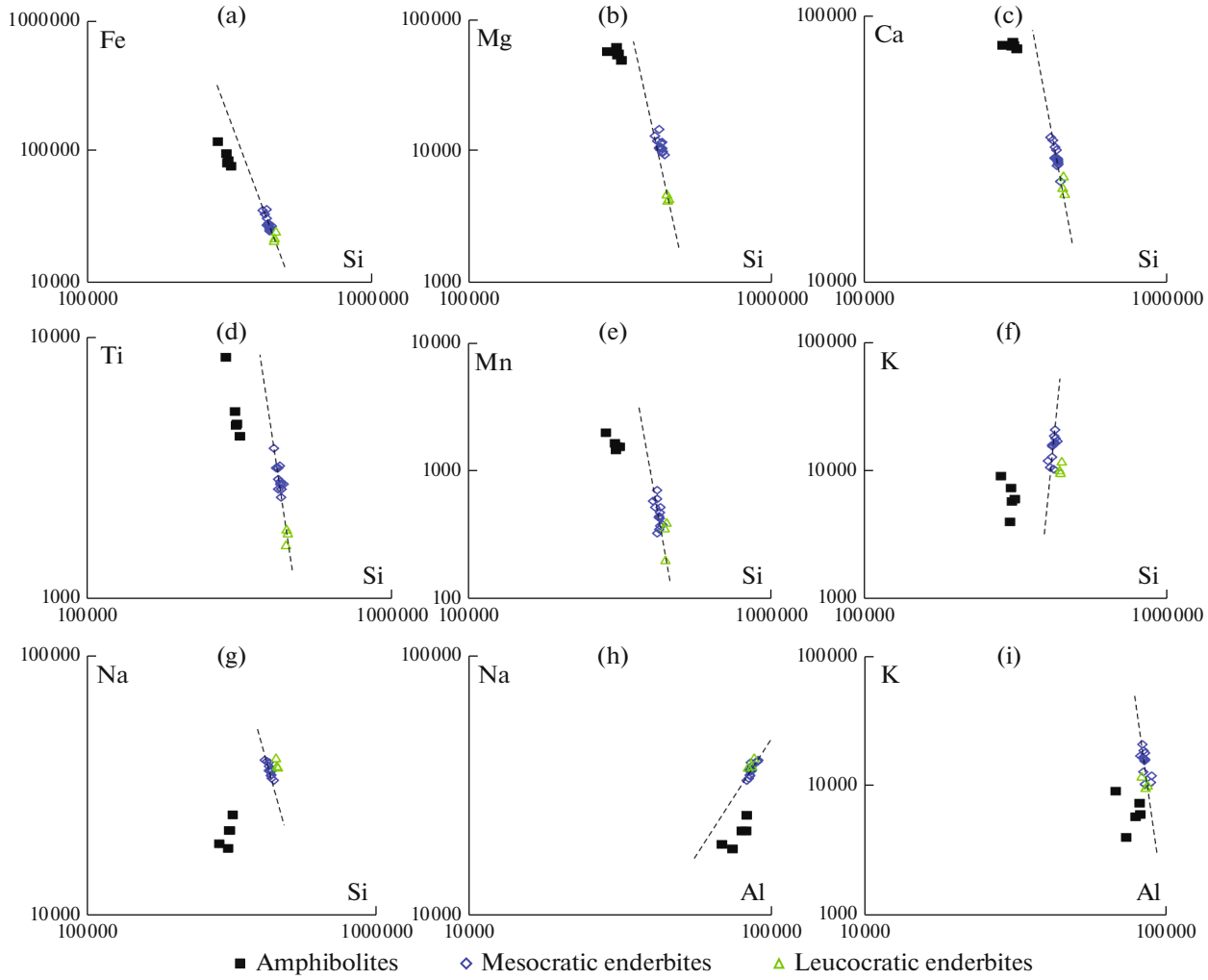

Fig. 3. Paired logarithmic ratios of major components and trace elements (ppm) in the enderbites of the Pon'goma-Navolok massif, illustrating the differentiation of the enderbite melt. Dashed lines show correlations in the enderbites, whereas the composition points of the amphibolites plot away from these lines.

display strong positive Si–K, Al–Na, and Ca–Mg correlations and negative Si–Na and Al–K ones (Figs. 4e, 4f, 4g, 4h, 4i). Thereby each of the rock groups (of both the enderbites and the charnockites) exhibits negative Si–Al, Si–Fe, Si–Mg, and Si–Ca correlations, but correlations between the enderbites and charnockites are disturbed (Figs. 4j, 4k, 4l). The charnockites are slightly richer in SiO_2 than the enderbites. These relations can be explained by the melting of the enderbites, introduction of Si and K with the metamorphic fluid, and complementary removal of Ca, Mg, and perhaps also Fe. This is reflected in that clinopyroxene ceases to be stable, and the contents of microcline increases in the charnockites, whose dominant Fe–Mg minerals are orthopyroxene, biotite, and titanomagnetite. Magnetite content in the charnockites is notably higher than in the enderbites: while the enderbites contain this mineral only as exsolution products in the ilmenite, the charnockites contain magnetite in the form of individual grains. The removal of Mg at charnockitization was more intense than Fe leaching from them, and hence, the Fe# of these rocks is remarkably higher than that of the enderbites: FeO/(FeO + MgO) = 0.62–0.87 (molar) versus 0.48–0.55 in the mesocratic enderbites of the main intrusive phase. Because magnetite is one of the principal Fe concentrators in the charnockites, these rocks show positive correlations in the pairs Fe–Mn, Fe–Ti, Fe–V, Fe–V, Ti–V, and Fe–Co.

In both the enderbites and the charnockites, REE strongly and positively correlate with P (Figs. 3h, 4d) and sometimes also with Ti, and this correlation is stronger for LREE than HREE. Inasmuch as the rocks contain apatite, the character of REE distribution in these rocks is controlled first of all by the behavior of this mineral.

Analysis of the REE patterns of the rocks indicates that the amphibolites, enderbites, and charnockites

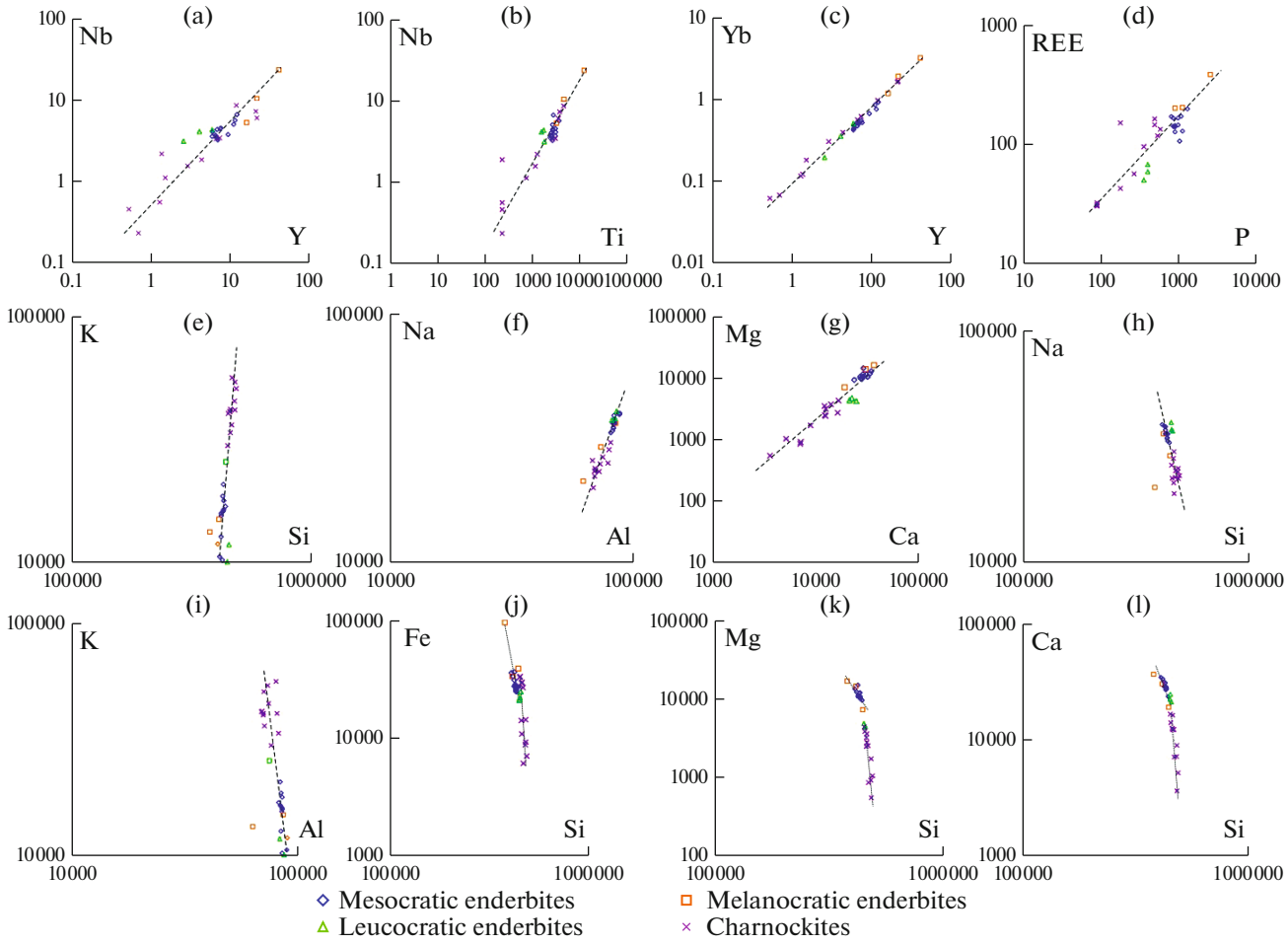

Fig. 4. Paired logarithmic ratios of major components and trace elements (ppm) in the enderbites of the Pon'goma-Navolok massif, illustrating that the charnockites could be derived from the enderbites under the effect of SiO_2- and K-rich fluid. Long dashed lines show common correlations for both the enderbites and the charnockites, and short-dashed lines show correlations of the separate compositional evolution of these rocks.

are obviously different. The amphibolites (Fig. 5) are characterized by gently sloped REE patterns, La/Sm(n) = 1.1–2.1, Gd/Yb(n) = 1.1–1.4, as is highly typical of BMB amphibolites not affected by Paleoproterozoic metamorphism and migmatization (Kozlovskii and Bychkova, 2015). In contrast to the amphibolites, the mesocratic enderbites of the main intrusive phase have differentiated REE patterns: they are enriched in LREE and depleted in HREE, with La/Sm(n) = 6.9–10.5 Gd/Yb(n) = 3.4–5.3 (Fig. 5).

The more differentiated character of the REE patterns of the enderbites compared to the amphibolites of the hypothetical protolith places some mineralogical constraints onto the parameters under which the enderbite melt was derived. First, the residue should have contained garnet as a concentrator of HREE. Second, LREE enrich apatite and amphibole and should have been preferably partitioned into the melt. Third, plagioclase as an Eu concentrator should also have been transferred into the melt but not remained in the residue, because otherwise the partial melts should have had a negative Eu anomaly, which is not the case. These mineralogical constraints make it possible to roughly outline the *P–T* field favorable for the derivation of the enderbite melt from the hypothetical amphibolite protolith.

The REE patterns of the enderbites define three clearly discernible groups (Fig. 6): (1) the melanocratic enderbites are most strongly enriched in REE and are characterized by a shallow Eu minimum with Eu/Eu* = 0.4–0.9; (2) the mesocratic enderbites of the main intrusive phase of the massif have intermediate REE patterns without Eu anomaly, Eu/Eu* = 0.9–1.3; and (3) the leucocratic enderbites are depleted in REE and do not have an Eu anomaly, Eu/Eu* = 1.0–1.3. The combination of the REE patterns and Eu behavior in the genetically related rocks of a single massif may likely be explained by the fractionation of plagioclase and accessory minerals (the most probable REE concentrators) in the magma

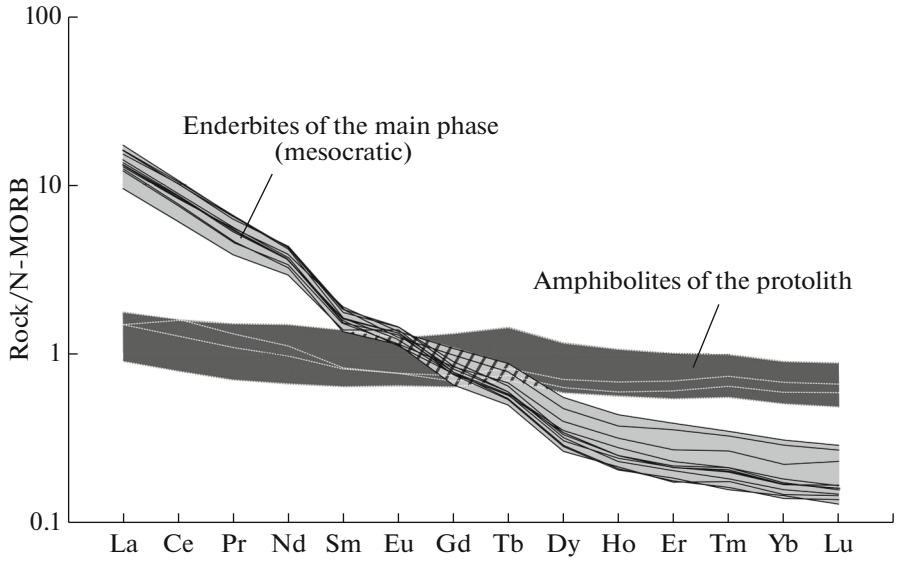

Fig. 5. REE patterns of the amphibolites and melanocratic enderbites of the main intrusive phase of the Pon'goma-Navolok massif. Here and below, REE patterns are normalized to N-MORB (Sun and Mc.Donough, 1989).

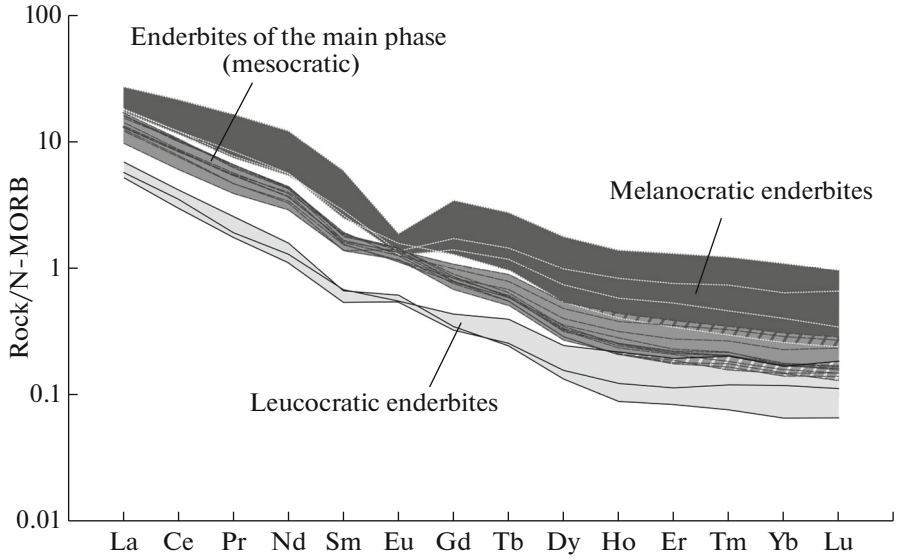

Fig. 6. REE patterns of the mesocratic, leucocratic, and melanocratic enderbites of the Pon'goma-Navolok massif.

chamber. The melanocratic enderbites (probable cumulates) are depleted in plagioclase and enriched in accessory minerals compared to the leucocratic and mesocratic enderbites. The later veined leucocratic enderbites are depleted in accessory minerals.

The configurations of the differentiated REE patterns make it possible to subdivide the charnockites into two sets (Fig. 7). One of them (set A) comprises the fine-grained charnockite dikes alone and is practically analogous to the mesocratic enderbites of the main phase: La/Sm(n) = 4.5–9.7, Gd/Yb(n) = 2.7–3.2, without clearly seen Eu anomaly. The other set (B) includes both the fine-grained and the pegmatoid charnockites, is notably depleted in both LREE and HREE, and its REE patterns are more differentiated: La/Sm(n) = 12.2–17.7, Gd/Yb(n) = 2.4–5.9, with a clearly seen positive Eu anomaly, Eu/Eu* = 1.9–3.7.

The occurrence of these two sets is likely explained by a low degree of melting of the enderbite protolith and different degrees of segregation of the charnockite melt. The integral effect of these two factors results in that the charnockite veins contain variable proportions of melted mobilized material and fragments of

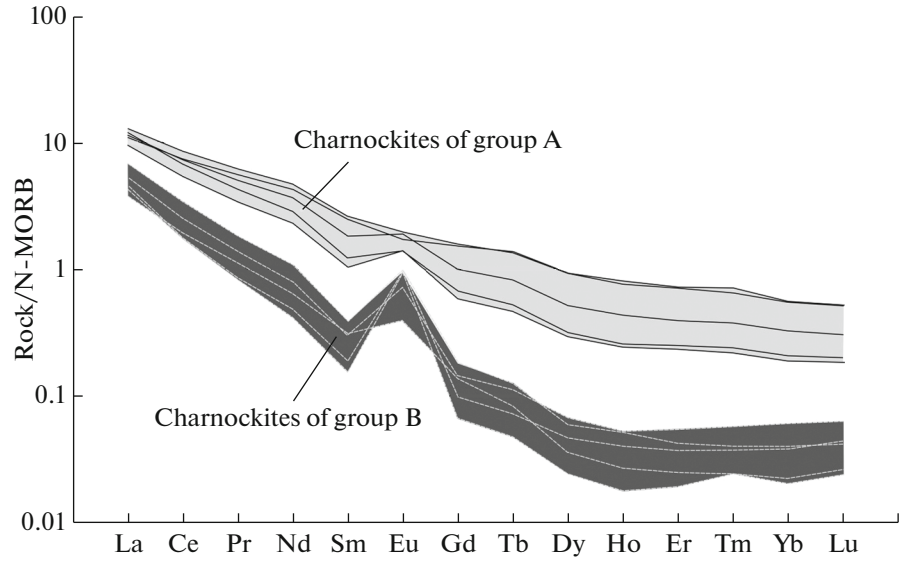

Fig. 7. REE patterns of the charnockites of the Pon'goma-Navolok massif.

the enderbite protolith. In the charnockites generated at a low degree of melting, melt segregation was insignificant, and hence, the newly formed melt was accumulated only in the intergranular space. Therewith the bulk REE composition corresponds to the enderbite protolith (origin of group-A charnockites). A higher degree of the segregation of the newly formed melt was related to the segregation of the partial melts from the enderbite protolith and the accumulation of the former in fractures. These charnockites are depleted in REE, except Eu (group-B charnockites).

Within the sheared domains, the development of Paleoproterozoic ductile flow zones was associated with the crystallization of the newly formed *Grt–Bt–Pl* association in the enderbites. The gneissose enderbites in contact zones of the massif become indiscernible in structure, texture, and mineralogy from TTG gneisses in the surroundings of the Pon'goma-Navolok massif. The REE patterns of the gneissose enderbites in the massif and orthogneisses in the surroundings of the massif make it possible to distinguish three groups of the rocks (normal, enriched, and depleted in REE), analogous to the melanocratic, mesocratic, and leucocratic enderbites (Fig. 8), although the boundaries between these groups are less clearly defined. The similarities of the REE patterns indicates that some types of the orthogneisses in the tonalite–trondhjemite–granodiorite complex of BMB may have been formed by shearing enderbites, and that REE were mostly inert in the course of Paleoproterozoic metamorphism in the absence of migmatization.

Some types of TTG orthogneisses in the surroundings of the massifs contain relics of clinopyroxene whose composition is close to that of clinopyroxene in the enderbites. G.M. Grugova (1996) described orthopyroxene in the host rocks of the massif. This provides further evidence that the enderbites served as the protolith of some types of the orthogneisses.

ISOTOPIC–GEOCHEMICAL FEATURES OF THE ENDERBITES, CHARNOCKITES, AMPHIBOLITES, AND APOAMPHIBOLITE GRANULITES OF THE PON'GOMA-NAVOLOK MASSIF

To identify the source of material from which the enderbites of the main phase of the Pon'goma-Navolok massif were derived, we used four samples of the most representative rocks of the complex: (1) enderbite of the main phase of the massif (sample PNG-58), (2) charnockite of the dike phase of the massif (sample PNG-113), (3) amphibolite from the largest block in the massif that has been least affected by granulite-facies metamorphism and recrystallization in the Paleoproterozoic ductile flow zones, and (4) apoamphibolite granulite from the block with the most widely spread orthopyroxene–clinopyroxene–plagioclase association. Results of the Sm–Nd and Rb–Sr isotope measurements are presented in Table 1. The calculated εNd(t) and $(^{87}Sr/^{86}Sr)_0$ are adjusted to the age of the massif: 2728 Ma (Levchenkov, 1996)

The high εNd (2728) and low $(^{87}Sr/^{86}Sr)_0$ values of all of the four analyzed rocks (Table 1) indicate that the rocks are genetically related to a depleted source. The data points of the enderbites and charnockites plot above the evolution line of the DM reservoir according to the model (Goldstein and Jacobsen, 1988) (Fig. 9). The range of the εNd values of the Archean amphibolites and metaultramafic rocks of the Central Belomorian Greenstone Belt determined on rocks from the Seryak structure (Slabunov, 2008) is

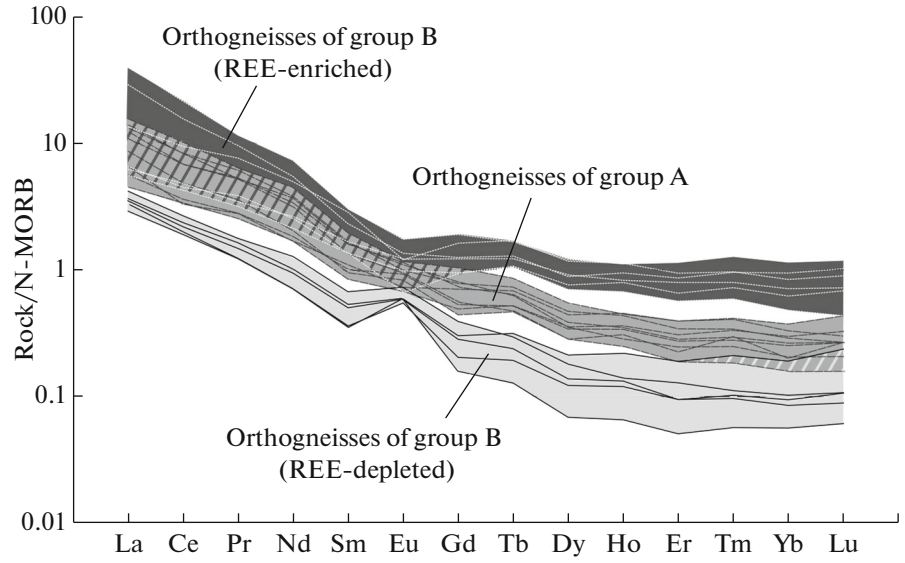

Fig. 8. REE patterns of garnet–biotite orthogneisses of various type in the surroundings of the Pon'goma-Navolok massif.

+2.2 to +4.5 (Fig. 9). The rocks of the Pon'goma-Navolok massif also fall within this range. The enderbites (sample PNG-58) and charnockites (sample PNG-113) have εNd (2728) = +4.3 and +4.4, respectively, and plot in the uppermost part of the range, whereas the amphibolites and apoamphibolite granulites (sample PNG-132) have εNd (2728) = +3.1 and +2.7 and plot in the lower part. The high εNd suggest that the enderbites of the Pon'goma-Navolok complex were melted off amphibolites with higher εNd values than those in the residual blocks within the massif. It can be hypothesized that the protolith of the enderbites was amphibolites at deeper crustal levels than the amphibolites currently accessible for observation and are hosted as blocks in the massif. Compared to them, the BMB amphibolites and metabasites that are also thought to had had an Archean protolith but crop out at the surface together with the orthogneisses of the TTG complex and have much lower εNd (2728), +1.6 and +2.6, as follows from our data (Fig. 9). The melts derived from these amphibolites would have not possessed such high εNd as in the rocks of the Pon'goma-Navolok massif.

The close spatial association of the enderbites and charnockites and their similar εNd (2728) = +4.3 and +4.4, respectively, suggest that the charnockites and enderbites were produced without any significant Nd introduction from an external source. However, the initial $(^{87}Sr/^{86}Sr)_0$ values calculated for an age of 2728 Ma increase in the succession amphibolite–granulite–enderbite–charnockite as 0.7008–0.7026–0.7031–0.7049 (Table 1) and reflect the systematic enrichment in radiogenic Sr. This enrichment seems to be explained by that the enderbites were melted from the amphibolites, and the charnockites were derived from the enderbites, with the involvement of metamorphic fluid that introduced some radiogenic Sr.

DISCUSSION: EVALUATION OF THE P–T–X_{CO_2}–X_{H_2O} PARAMETERS UNDER WHICH THE SILICIC MELTS OF THE PON'GOMA-NAVOLOK MASSIF WERE GENERATED

The chemical composition of the enderbites, geochemical correlations between elements in the enderbites and amphibolites (Figs. 1–3), and isotopic–geochemical features of rocks of the Pon'goma-Navolok complex led us to conclude that some types of BMB amphibolites may have been the probable protolith for

Table 1. Sm–Nd and Rb–Sr isotope data on the studied rocks of the Pon'goma-Navolok massif

Sample	Sm, ppm	Nd, ppm	$^{147}Sm/^{144}Nd$	$^{143}Nd/^{144}Nd$	±2σ	Rb, ppm	Sr, ppm	87Rb/86Sr	±2σ	$^{87}Sr/^{86}Sr$	±2σ	εNd (2728)	$(^{87}Sr/^{86}Sr)_0$ (2728)
PNG-58	8.08	46.10	0.1059	0.511225	±19	13.3	835.6	0.0460	0.00002	0.704905	±18	+4.3	0.703088
PNG-113	3.06	14.41	0.1285	0.511633	±8	84.4	555.8	0.4399	0.0001	0.722319	±9	+4.4	0.704944
PNG-123	1.65	4.84	0.2063	0.512969	±11	15.8	111.3	0.4107	0.0001	0.717046	±10	+3.1	0.700824
PNG-132	2.18	7.31	0.1800	0.512477	±5	3.5	178.7	0.0569	0.00002	0.704816	±7	+2.7	0.702569

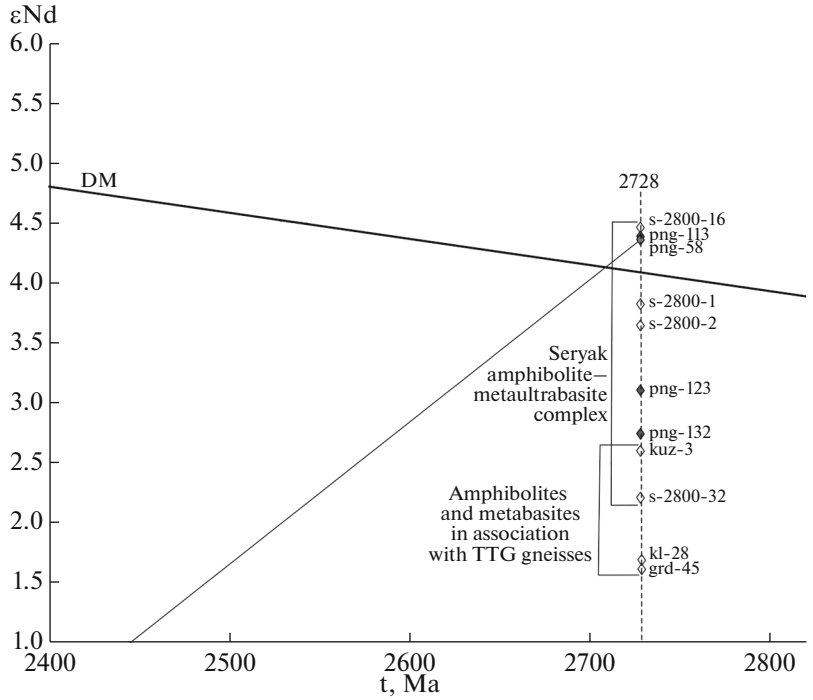

Fig. 9. Evolution of the Nd isotopic composition in the enderbite–charnockite Pon'goma-Navolok complex. Solid symbols are rocks of the Pon'goma-Navolok complex (samples: PNG-58 enderbite, PNG-113 charnockite, PNG-123 amphibolite, PNG-132 apoamphibolite mafic granulite). Open symbols are metabasites from other BMB areas for which an Archean protolith was hypothesized. Samples from the Seryak complex (Slabunov, 2008): S-2800-16 amphibolite, S-2800-1 and C-2800-32 garnet amphibolites, C-2800-2 ultramafic rock. Our samples (Kozlovskii et al., 2019) of the association of metabasites with orthogneisses from the middle reaches of the Verkhnyaya Kuzemka River and Kemluda Islands: KUZ-3 eclogite-like rock, KL-28 apoamphibolite eclogite, GRD-45 amphibolite from Kochkova Island, our unpublished data.

silicic melts whose composition was close to that of the phase-I enderbites of the Pon'goma-Navolok massif. Such melts could be melted off the amphibolites under the effect of metamorphic fluid rich in K, Na, and SiO_2. The probable protolith for the phase-II charnockites may have been the phase-I enderbites of this massif. To derive melts of composition close to the charnockites, the enderbites should have been affected by fluid rich in K and SiO_2.

The model for the generation of acid melt in the amphibolites is based on the process of amphibolite melting in the presence of saline H_2O–CO_2 fluid under parameters of the lower crust. The melting of amphibolite was modeled by minimizing the Gibbs free energy (method of pseudosections) with the use of the PERPLE_X 6.8.7. program package (Connoly, 2005), in the system SiO_2–Al_2O_3–FeO–MgO–CaO–Na_2O–K_2O–O_2–H_2O–CO_2–NaCl. The model composition chosen for the simulations was that of amphibolite from a large block within the massif (sample PNG-123). The following models of mineral solid solutions were used: feldspar (Fuhrman and Lindsley, 1988), *Opx*(W) and *Gt*(W) (White et al., 2014), *Cpx*(HP) (Holland and Powell, 1996), *Amph*(DHP) (Dale et al., 2000), and the melt(G) model of tonalite melt (Green et al., 2016).

First, phase relations were modeled for amphibolite melting in the absence of a fluid phase. The modeled compositions were poorer in SiO_2 than the enderbites. Based on the aforementioned geochemical correlations, which indicate that the derivation of the enderbites requires SiO_2 introduction, we assumed that SiO_2 and H_2O are excess components, and the system is saturated with them. The assumed fluid components were H_2O, CO_2, and NaCl, whose mixing properties were calculated based on the model (Aranovich et al., 2010).

The main set of the calculations was thus conducted with regard to that the system is oversaturated with SiO_2 and that melting proceeds in the presence of H_2O–CO_2–NaCl fluid. The calculations were carried out at 0.07, 0.15, 0.20, 0.30, and 0.40 NaCl mole fractions in the fluid. The concentration of free O_2 as a parameter reflecting Fe_2O_3 concentration in the system was also specified as discrete values: 0.10, 0.12, and 0.20 wt %. For each NaCl mole fraction in any P–T pseudisection, the pressure was preparatorily evaluated. For any obtained pressure value in a T–X_{CO_2} pseudisection, the CO_2 mole fraction in the fluid was evaluated, and then corrected pseudosections were plotted in P–T space for this CO_2 content, and the values of

Table 2. Calculated $P–T–X_{CO_2}–X_{NaCl}$ parameters favorable for the derivation of the enderbite melts (modeling results). Numerals in parentheses are values for the average mesocratic enderbite (11 samples)

X_{NaCl}	X_{CO_2}	P, kbar	T, °C
0.00	0.34–0.46	**13.0–15.8**	**1040–1070**
	(0.41) average enderbite	(14.8) average enderbite	(1060) average enderbite
0.07	0.25–0.38	**13.0–15.5**	**1050–1075**
	(0.33) average enderbite	(14.9) average enderbite	(1060) average enderbite
0.15	0.17–0.30	**12.5–15.7**	**1040–1070**
	(0.24) average enderbite	(14.9) average enderbite	(1060) average enderbite
0.20	0.09–0.25	**13.1–15.6**	**1040–1070**
	(0.20) average enderbite	(14.6) average enderbite	(1060) average enderbite
0.30	0.03–0.16	**12.8–15.8**	**1040–1080**
	(0.10) average enderbite	(14.8) average enderbite	(1060) average enderbite
0.40	0.00–0.08	**12.9–15.6**	**1030–1080**
	(0.02) average enderbite	(14.8) average enderbite	(1060) average enderbite

these parameters were determined. If necessary, the calculations were repeated. Corrections for O_2 content were introduced during the final stage, but it did not any significantly modify the fields of mineral assemblages[4].

The $P–T$ parameters of the stability of the enderbite melt were constrained by finding intersections (superpositions) of the isopleth of the molecular ratios $al = Al_2O_3/(Al_2O_3 + FeO + MgO + CaO)$, $fm = (FeO + MgO)/(Al_2O_3 + FeO + MgO + CaO)$, and $ca = CaO/(Al_2O_3 + FeO + MgO + CaO)$ for the model melt *melt(G)* corresponding to the composition of the naturally occurring enderbite $al = 0.46–0.51$, $fm = 0.28–0.30$, $ca = 0.20–0.24$ (Figs. 10a, 10b). If the model is inconsistent with the real rock compositions, the region of isopleth superpositions cannot be outlined. Proportions involving SiO_2, Na_2O, and K_2O were not used to constrain the field of the enderbite melt. The regions outlined using the isopleths include 11 to 13 analyses of the main-phase mesocratic enderbites. These regions occur in the $P–T$ stability field of orthopyroxene *Opx*(W), clinopyroxene *Cpx*(HP), and garnet *Grt*(W), whereas plagioclase (feldspar) and amphibole *Amph*(DHP) are absent from this field (Fig. 10b). This is consistent with the mineralogical constraints identified by analyzing the REE patterns.

The field *melt*(G) + *Opx*(W) + *Cpx*(HP) + *Grt*(W), in which the best convergence of the molecular ratio lines occurred, can be interpreted as the stability field of the melt and residue. The content of melt in this field varies within the range of 45–67 vol % (Fig. 10c). At lower temperatures, outside the stability field of the melt (line *melt+/melt–* in Fig. 11b) at $T = 930–950$°C, the mineral association additionally involves plagioclase, and the melt content therewith significantly decreases to 0–40 vol %. This field corresponds to granulite-facies migmatites. The field *Opx*(W) + *Cpx*(HP) + *Grt*(W) + *feldspar* (Fig. 10b), which corresponds to the garnet–orthopyroxene–clinopyroxene granulites that can be regarded as the host rocks, occurs at a temperature of 870–930°C

Figures 10a–10c show results only at a NaCl mole fraction, X_{NaCl}, in the fluid equal to 0.15. Analogously we have calculated the $T–X_{CO_2}$ and $P–T$ pseudosections corresponding to $X_{NaCl} = 0.00$, 0.07, 0.20, 0.30, and 0.40. In these pseudosections, regions of $P–T–X_{CO_2}$ values at which amphibolite melting in the presence of saline $H_2O–CO_2$ fluid could most probably result in melts similar in composition to the enderbites of the Pon'goma-Navolok massif were determined from the best consistency of the isopleths of cation proportions in the melt at each X_{NaCl}. Results of these calculations are presented in Table 2 and Fig. 11.

These data indicate that the $P–T$ parameters favorable for the derivation of these melts are 12.5–15.8 kbar (average 14.8 kbar) and 1030–1080°C (average 1060°C). However, the X_{CO_2} and X_{NaCl} in the fluid show a strong negative correlation. This indicates that the fluid favorable for the derivation of the enderbites should have had a low H_2O activity, regardless of the reason for this: whether it was a high concentration of salts or CO_2.

Using data from Table 2, fluid compositions favorable for the derivation of enderbites are outlined in the $H_2O–CO_2–NaCl$ diagram of phase relations (Aranovich et al., 2010) (Fig. 11). Most of this field lies within the region of two coexisting fluids under a pressure of 9 kbar. However, the field of homogeneous fluid expands with increasing pressure, and hence, it is

[4] The optimal O_2 content in the system was evaluated at 0.12 wt %. At lower O_2 contents, the intersections of isopleths of the melt occur where garnet is not stable, which is in conflict with the mineralogical constraints determined above from the REE distributions. At higher O_2 contents, clinopyroxene containing relatively much acmite (13 mol % and more) is stable, which is atypical of this complex.

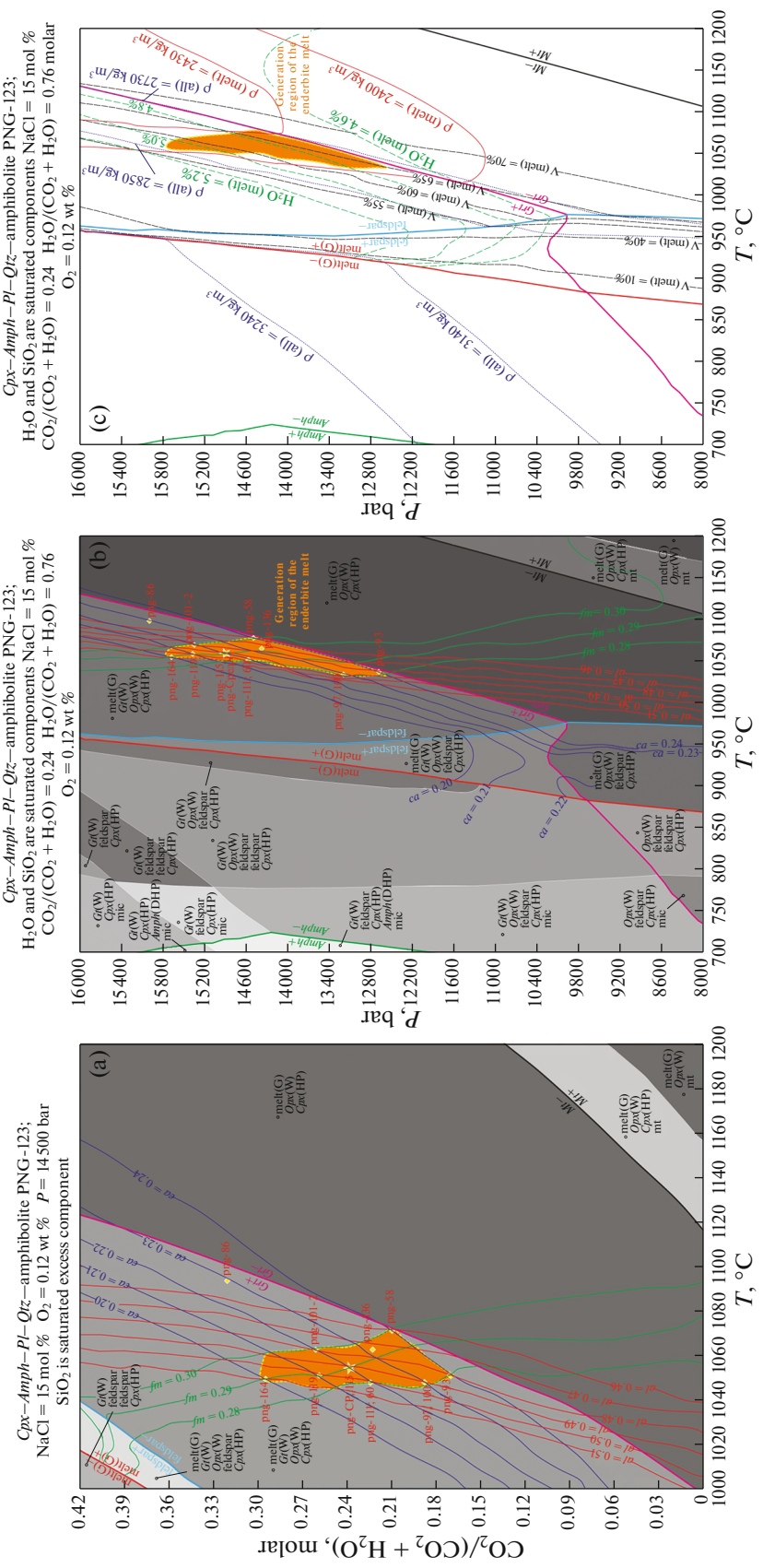

Fig. 10. Pseudosections illustrating the region favorable for the melting of the amphibolites: (a) in T–CO_2 space, (b) in P–T space, (c) isopleths of density, volume, and H_2O content in the model melt in P–T space. In Figs. 10a and 10b, red, green, and blue lines show isopleths of cation ratios in the phase *melt*(G). The orange field is the region of isopleth convergence, which corresponds to the derivation region of melt of composition close to that of the main-phase enderbite. Yellow lozenges and labels near them are real enderbite compositions (see Supplementary). The yellow star is the average of 11 analyses.

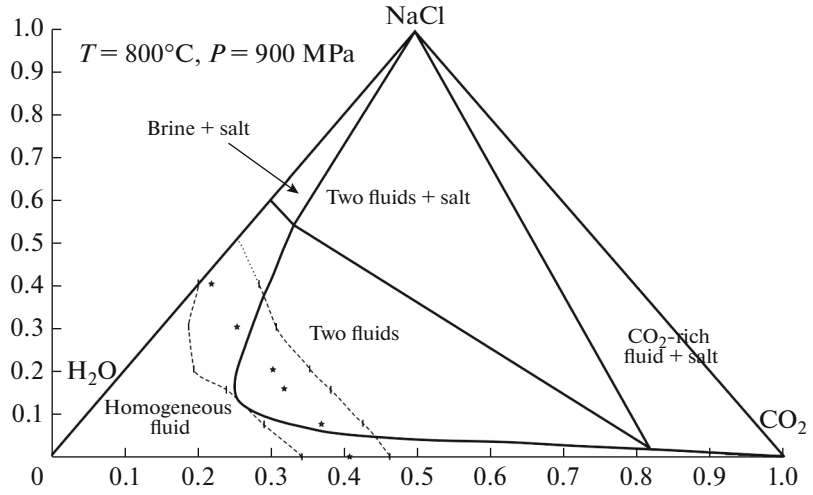

Fig. 11. Phase relations in the CO_2–H_2O–NaCl system (Aranovich et al., 2010) at a pressure of 9 kbar. The dashed line contours the region of fluid compositions in equilibrium with enderbite melts in their generation region, evaluated based on the whole set of rock analyses. Stars are the same based on the average enderbite composition (see Table 2).

reasonable to anticipate that homogeneous saline H_2O–CO_2 fluid can occur at P = 12.5–15.8 kbar, i.e., the parameters at which the enderbite melt was derived. The model melt contained 4.7–5.1 wt % H_2O in this P–T region (Fig. 10c).

Water activity in the fluid was evaluated using T–log(a_{H_2O}) pseudosections and by plotting al = $Al_2O_3/(Al_2O_3 + FeO + MgO + CaO)$ = 0.46–0.51, fm = (FeO + MgO)/(Al_2O_3 + FeO + MgO + CaO) = 0.28–0.30, and ca = CaO/(Al_2O_3 + FeO + MgO + CaO) = 0.20–0.24) isopleths. One of the pseudosections at X_{NaCl} = 0.15 and a pressure of 14.9 kbar is shown in Fig. 12. The diagram demonstrates that the melts derived at 1030–1080°C can have a composition close to that of the enderbites of the Pon'goma-Navolok massif only at log(a_{H_2O}) = –0.47 to –0.32 for all of the analyses (–0.42 for the average enderbite), which translates to a_{H_2O} = 0.34–0.48 (0.38 for the average enderbite composition). The field in which the enderbite melt was derived is adjacent to the garnet stability field. Because of this, melting at a higher H_2O activity should have proceeded in the absence of garnet, and such a melt should not have a differentiated REE pattern. A lower H_2O activity, less than 0.18, should have shifted the compositions of the partial melts into the stability field of plagioclase in the residue, which should have led to an Eu minimum in the respective REE patterns.

The isopleths in Fig. 12 indicate that melts derived within the garnet stability field could have been generated at a lower temperature and/or higher water activity. However, the composition of these melts should differ from those of the enderbites of the Pon'goma-Navolok massif: these melts should be more aluminous and contain less Ca, Fe, and Mg.

The amount of enderbite melts in its generation region is 57–67 vol % (Fig. 10c), and its density ρ = 2400–2430 kg/m^3. The density of the melt + residue system as a whole is notably higher: ρ = 2730–2850 kg/m^3, which results in a gravitational instability of this system. However, the densities should be more accurately compared not in the melt–residue system but in the system melt–unmelted host rocks. The latter may have been the garnet–clinopyroxene–orthopyroxene–plagioclase granulites (*Grt* + *Opx* + *Cpx* + *feldspar*), whose field is adjacent (on the right-hand side, at lower temperatures) to the generation region of the melt (Fig. 10b). The density of such granulites under a pressure of 12.5–15.8 kbar at temperature of 920–930°C is 3140–3240 kg/m^3 (average 3190 kg/m^3), i.e., these rocks are much heavier than those affected by partial melting. The notable (by a factor of 1.3) difference between the densities of the host rocks and autochthonous melt and the great volume of the partial melts (57–67 vol %) led us to suggest that the melt could have been separated from its generation region and migrated through tectonized extension zones to higher crustal levels as mixture of melt + residual minerals. However, the enderbites contain no residual phases, primarily garnet[5], and the compositions of the dominant rock-forming minerals (plagioclase and orthopyroxene) are usually close to the equilibrium compositions with the melt (assumed as the bulk composition of the rock) under P–T parameters of its crystallization but not melting (Kozlovskii et al., 2022). Because of this, when the enderbite melt ascended to higher crustal levels along fractures, residual minerals were practically not removed from the melting region.

[5] The only likely residual mineral of the enderbites is low-Fe [FeO/(FeO + MgO) = 0.28–0.3] clinopyroxene, which occurs in minor amounts.

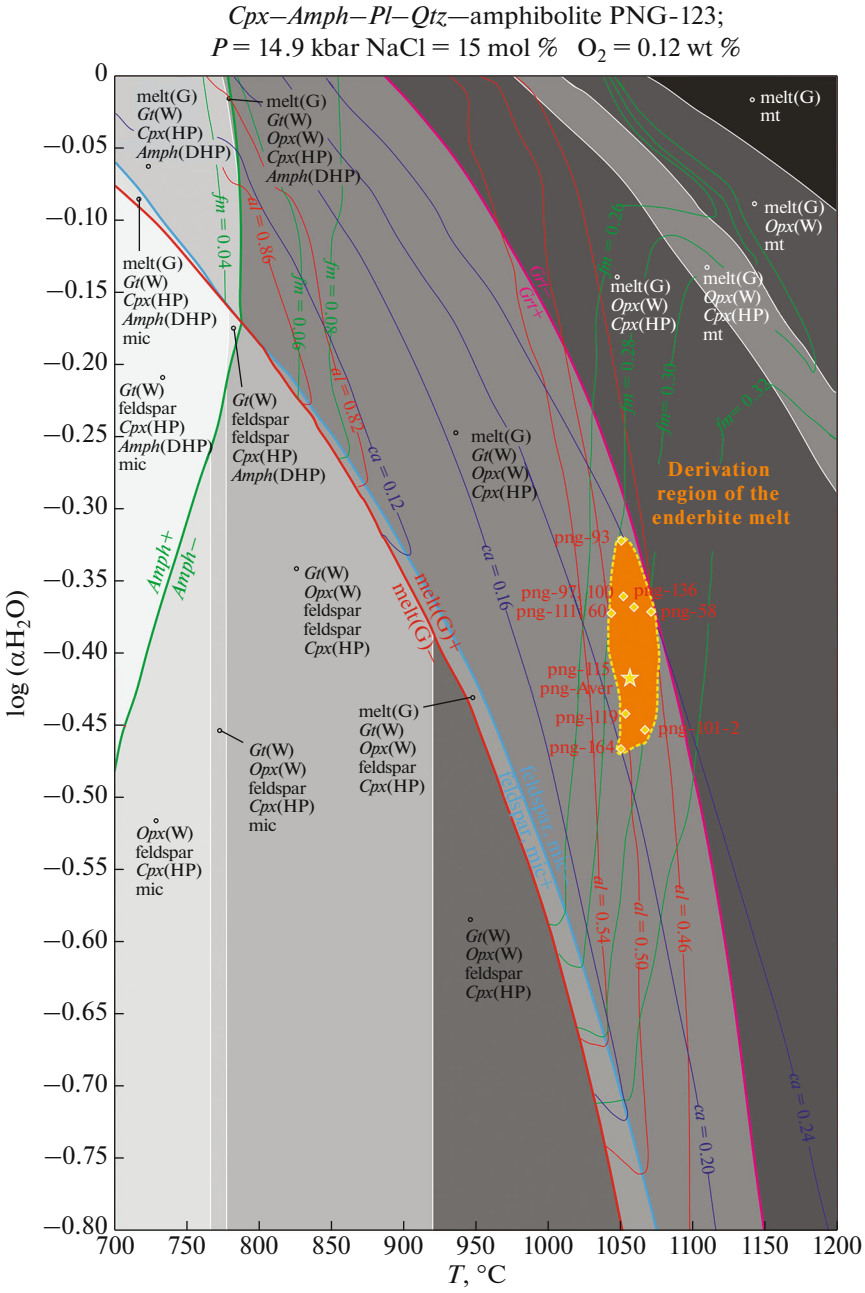

Fig. 12. T–log(a_{H_2O}) pseudosection showing the region favorable for the derivation of the enderbite melt from amphibolite. The orange field is the region of the maximum superposition of cation ratios in the model melt *melt*(G), corresponding to real enderbite compositions; the field corresponds to the derivation region of melt of composition close to that of the main-phase enderbites. Yellow lozenges and labels near them are real analyses of the enderbites (see Supplementary for analyses). The yellow star is the average of 11 analyses.

We believe that this mechanism of melt ascent is more typical of orogens evolving in a convergent regime.

According to the model (Persikov and Bukhtiyarov, 2009), the viscosity of enderbite melt with 5% H_2O at P = 14.8 kbar and T = 1060°C is $\eta = 5.87 \times 10^2$ Pa s. This relatively low viscous melt could have bee readily forced off along fractures and pooled to form massifs at higher crustal levels (at which the viscosity of the melts increased because of their dehydration and the pressure decrease). It is hard to expect that large enderbite massifs could be formed at depths corresponding to 15 kbar, but zones of veined enderbite migmatization in TTG gneisses were documented in the vicinities of the village of Gridino, which is the

highest pressure segment of BMB (Sibilev et al., 2013), and where metamorphic rocks crop out that were formed under pressures of 15–17 kbar (according to our data) and more.

Table 2 and Fig. 10b show that melts of composition close to the enderbites could be derived only at pressures of 12.5–15.8 kbar, which correspond to notably greater depths than those calculated for the metamorphism of the amphibolite blocks hosted in the enderbite (their metamorphic pressure was evaluated at 8.3–10.0 to 10.3–11.0 kbar). A rough estimate of the depths at which the enderbites were derived, with regard to the density of the whole system $\rho = 3190$ kg/m^3, is 40–50 km, which corresponds to the lower crust or the crust/mantle boundary. The melting temperature of the enderbites is 1030–1080°C, i.e., was much higher than the peak metamorphic temperatures of the metabasite blocks (830–910°C). Thus, the generation region of the enderbite melt and the parameters of granulite-facies metamorphism of the amphibolite blocks differ in both pressure and temperature. No partial enderbite melts could be derived at the metamorphic parameters in the blocks (if this metamorphism is thought to be of regional nature). This controversy can be eliminated if the granulite-facies metamorphism in the amphibolite blocks is assumed to be of contact nature, under the thermal effect of the enderbite massif. Hence, the apoamphibolite clinopyroxene–orthopyroxene granulites in the amphibolite blocks hosted in the enderbites should be regarded as contact hornfels. However, garnet–clinopyroxene–orthopyroxene–plagioclase granulites and corresponding migmatites produced at lower temperatures than those in the melting region of the enderbites may be regionally widespread at depths corresponding to pressures of 12.5–15.8 kbar (Fig. 10b).

Comparison of the pressure and temperature evaluations and the depths at which the enderbite chamber was formed with the configuration of geotherms in Precambrian complexes, obtained by numerical simulations of subduction (Perchuk et al., 2019) and collision (Perchuk et al., 2018), led us to conclude that temperatures of 1000–1100°C cannot be reached at depths of 40–50 km in stable tectonic blocks. In the undeformed oceanic or continental crust, this depth corresponds to geotherms of 500–700°C (marginal parts of the model blocks). An elevated heat flow resulting in the ascent of geotherms can be reached only in a small part of the suprasubductional region (in the model of hot Precambrian subduction, $\Delta T = 150$°C) or in the central portion of an orogenic edifice above melting regions in the mantle (in the model of a Precambrian hot orogen during its final evolution). An important condition for the ascent of geotherms and operation of high-temperature granulite-facies metamorphism is, according to model calculations, a small thickness of the continental crust. In the Precambrian geological history of BMB, it was at 2728 Ma (which is the age of the enderbites) when its subduction–accretion evolutionary phase ended at 2.74–2.72 Ga (Slabunov and Sibilev, 2008) and the precollisional evolutionary phase began at 2.73–2.72 Ga (Slabunov, 2008). Thus, the thick continental crust of BMB was formed notably later, at 2.217–2.58 Ga (Slabunov, 2008), and it did not hamper the ascent of geotherms, high-temperature metamorphism, and the melting of the amphibolites.

CONCLUSIONS

(1) The main-phase enderbites of the Pon'goma-Navolok massif were produced by magma that had been derived (melted) from an amphibolite protolith in the presence of saline H_2O–CO_2 fluid with a low H_2O activity. The magma was derived in the presence of garnet in the residue, and this led to the depletion of the partial enderbite melts in HREE compared to the protolithic amphibolite.

(2) The protolith of the enderbite melts may have been the amphibolites of the Archean greenstone belts in BMB, which had characteristics of a depleted source. The enderbites and charnockites show no evidence of their crustal contamination.

(3) The P–T field favorable for the derivation of the partial melts of composition close to the main-phase enderbites of the massif occurred at a depth of 40–50 km, which roughly corresponds to the lower crust or crust/mantle boundary at $P = 12.5$–15.8 kbar (average 14.8 kbar). The temperatures of 1030–1080°C (average 1060°C) at which the enderbite melts were derived imply that additional heat flow occurred, as is typical of crust and upper mantle during the final evolution of hot orogens.

(4) The fractionation of plagioclase and accessory minerals during the crystallization of the enderbites of the main phase in a magma chamber is reflected in the geochemistry of the rocks and their mineralogy. Plagioclase enrichment in the leucocratic enderbites resulted in their depletion in REE and in Eu anomalies of these rocks. The depletion of plagioclase and accessory minerals in the melanocratic enderbites was associated with an increase in REE concentrations and in negative Eu anomalies.

(5) Although the rocks are gneissose and were affected by high-pressure metamorphism when the Paleoproterozoic ductile flow zones were formed and overprinted the enderbites of the Pon'goma-Navolok massif, these rocks have preserved features of REE distributions typical of the primary magmatic rocks of the massif. The gneissose enderbites and TTG gneisses in the surroundings of the massif can be subdivided into three rock types according to the degrees of their enrichment in REE: meso-, melano-, and leucocratic enderbites. This indicates that the enderbites analogous to the rocks of the Pon'goma-Navolok massif may have been the protolith of some types of the orthogneisses.

(6) The enderbite melts were derived at notably higher P–T parameters, 12.5–15.8 kbar and 1030–1080°C, than those of the clinopyroxene–orthopyroxene–plagioclase peak metamorphic associations of the apoamphibolite granulite-facies metamorphism in amphibolite blocks in the massif: 830–910°C and 10.3–11.0 kbar. At the modern erosion level, corresponding to the middle crust, granulite-facies metamorphism could not induce partial melting at temperatures more than 100°C higher than the peak metamorphic temperature and a much greater depth. However, the emplacement of enderbites and their crystallization at 8.1–11.4 kbar and 925–970°C could well initiate granulite-facies metamorphism in the contact aureole of the massif and in rock blocks within the massif. Because of this, granulite-facies metamorphism at the modern erosion level in Belomorie was likely of contact, but not regional, nature. This is consistent with the homogeneous (hornfels) texture of the granulites, which is atypical of regional metamorphic rocks.

ACKNOWLEDGMENTS

The authors thank S.A. Silantyev, O.G. Safonov, and O.M. Turkina for valuable comments, discussions of the principal results of this study, and help with the preparation of the manuscript. The authors are thankful to the staff of the ANALYTIC Center for the Collective Use of Analytical Equipment at IGEM RAS for conducting XRF analyses of rock samples.

FUNDING

This study was carried out under government-financed research project for IGEM RAS and was supported by the Russian Science Foundation, Grant RNF-23-17-00066. The Rb–Sr and Sm–Nd isotope data were acquired under government-financed research project for GEOKHI RAS.

CONFLICT OF INTEREST

The authors declare that they have no conflicts of interest.

OPEN ACCESS

SUPPLEMENTARY INFORMATION

The online version contains supplementary material available at https://doi.org/10.1134/S0016702923090069.

REFERENCES

L. Y. Aranovich, I. V. Zakirov, and N. G. Sretenskaya, "Ternary system H_2O–CO_2–NaCl at hight parameters: an mixing model," Geochem. Int. **48** (5), 446–455 (2010).

V. S. Baikova, I. S. Sedova, and I. K. Shuleshko, "Composition of minerals in grantoids suffered to the polymetamorphism (Belomorian–Lapland Belt, Pongoma area)," Zap. Ross. Mineral. O-va **130** (3), 94–113 (2001).

V. S. Baikova, E. S. Bogomolov, and T. F. Zinger, "Basite dikes of Pongom–Navolok Island (Belomorian–Lapland Belt)," Zap. Ross. Mineral. O-va **134** (4), 108–116 (2005).

J. A. Connolly, "Computation of phase equilibria by linear programming: a tool for geodynamic modeling and its application to subduction zone decarbonation," Earth Planet. Sci. Lett. **236** (1–2), 524–541 (2005).

J. Dale, T. Holland, and R. Powell, "Hornblende-garnet-plagioclase thermobarometry: a natural assamblege calibration of the thermodynamics of hornblende," Contrib. Mineral. Petrol. **140**, 153–362 (2000).

G. M. Drugova, "Early Precambrian metamorphism in the Belomorian orogenic belt (Baltic shield), Zap. Ross. Mineral. O-va **125** (2), 24–37 (1996).

G. M. Drugova, L. V. Klimov, and M. D. Krylova, "Early stages of granulite metamorphism in the Belomorian Complex," Dok. Akad. Nauk SSSR **234** (3), 665–668 (1977).

G. M. Drugova, E. Yu. Borisova, and Sh. K. Baltybaev, "Two stages of granulitic metamorphism in Archean garnet gneisses of the White Sea folded belt, Baltic Shield," Dokl. Earth Sci. **357** (1), 1161–1164 (1997).

B. R. Frost, C. G. Barnes, W. J. Collins, R. J. Arculus, D. J. Ellis, and C. D. Frost, "A geochemical classification for granitic rocks," J. Petrol. **42** (11), 2033–2048 (2001).

M. L. Fuhrman and D. H. Lindsley, "Ternary-feldspar modeling and thermometry," Am. Min. **73** (3–4), 201–215 (1988).

S. J. Goldstein and S. B. Jacobsen, "Nd and Sr systematics of river water suspended material implication for crustal evolution," Earth Planet. Sci. Lett. **87** (3), 249–268 (1988).

E. C. R. Green, R. W. White, J. F. A. Dener, R. Powel, T. J. B. Holland, and R. M. Palin, "Activity-composition relations for the calculation of partial melting equilibria in metabasic rocks," J. Metamorph. Geol. **34** (9), 845–869 (2016).

T. Holland and R. Powell, "Thermodynamics of order-disorder in minerals. II. Symmetric formalism applied to solid solutions," Am. Mineral. **81** (11–12), 1425–1437 (1996).

S. B. Jacobson and G. J. Wasserburg, "Sm-Nd isotopic evolution of chondrites and achondrites," Earth Planet. Sci. Lett. **67** (2), 137–150 (1984).

N. E. Korol, "Mafic granulites of Karelia and Central Finland," Geol. Polezn, Iskop. Karelii. Tr. Karel'sk. Nauchn. Ts. RAS **8**, 18–39 (2005).

N. E. Korol, "High-Temperature amphibolization synchronous with enderbite migmatization of mafic granulites in granulite–enderbite–charnockite complexes in Karelia," Petrology **17** (4), 352–370 (2009).

N. E. Korol, "Late isofacies recrystallization in the granulite–enderbite–charnockite complexes of Karelia," Geol. Polezn, Iskop. Karelii. Tr.Karel'sk. Nauchn. Ts. RAS **14**, 8–32 (2011).

N. E. Korol, "Metamorphic evolution of the Pongom-Navolok granulite–enderbite–charnockite complex of the Belomorian mobile belt," Geol. Polezn, Iskop. Karelii. Tr. Karel'sk. Nauchn. Ts. RAS **11**, 34–56 (2018).

L. A. Kosoi, "Archean limestones and genesis of the Belomorian sequence of Karelia," Uch. Zap. Lening. Gos. Univ. Ser. Geol.-Pochv.-Geograf. Vyp 3. Zemnaya kora **2** (10), 53–79 (1936).

Yu. A. Kostitsyn and D. Z. Zhuravlev, "Analysis of errors and optimization of isotope dilution method," Geokhimiya, No. 7, 1024–1036 (1987).

V. M. Kozlovskii and Y. V. Bychkova, "Geochemical evolution of amphibolites and gneisses of the Belomorian mobile belt during paleoprotrrozoic metamorphism," Geochem. Int. **54** (6), 529–542 (2016).

V. M. Kozlovskii, V. M. Savatenkov, L. B. Terenteva, and E. B. Kurdyukov, "First data on Yatulian (2.1 Ga) metamorphism in the Belomorian Mobile Belt," Dokl. Earth Sci. **485** (3), 322–326 (2019).

V. M. Kozlovskii, V. V. Travin, T. F. Zinger, E. B. Kurdyukov, I. S. Volkov, and M. A. Yakushik, "Metamorphism of basites in zones of ductile flow and beyond their limits," *Rock-Mineral and Ore Formation: Progress and Prospects in Study. Proc. All-Russian Conf. with International Participation Dedicated to the 90th Anniversary of IGEM RAS* (IGEM RAS, Moscow, 2021), pp. 345–348 [in Russian].

V. M. Kozlovskii, V. V. Travin, T. F. Zinger, E. B. Kurdyukov, and M. A. Yakushik, "Archean charnockite–enderbite complexes of the Belomorian zone. Origin and conditions of melt generation," Geol. Polezn. Iskop. Karelii. Tr. Karel'sk. Nauchn. Ts. Ross. Akad. Nauk, No. 5, 55–59 (2022).

O. A. Levchenkov, T. F. Zinger, V. L. Duk, S. Z. Yakovleva, V. S. Baikova, I. K. Shuleshko, and D. I. Matukov, "U–Pb zircon age of the hypersthene diorites and granodiorites of Pon'gom-Navolok Island (Baltic Shield, White Sea Tectonic Zone)," Dokl. Earth Sci. **349** (1), 852–854 (1996).

L. K. Levsky, I. M. Morozova, O. A. Levchenkov, V. S. Baikova, and E. S. Bogomolov, "Isotopic-geochronological systems in metamorphic rocks: Pongoma island, Belomorian mobile belt," Geochem. Int. **47** (3), 215–230 (2009).

K. R. Ludwig, "User's Manual for Isoplot / Ex, Version 3.00: A geochronological toolkit for Microsoft Excel," Berkeley Geochronol. Center. Spec. Publ., No. 4, (2003).

A. L. Perchuk, O. G. Safonov, C. A. Smit, V. S. Zakharov, and T. V. Gerya, "Precambrian ultra-hot orogenic factory: Making and reworking of continental crust," Tectonophysics **746**, 572–586 (2018).

A. L. Perchuk, V. S. Gerya, T. V. Zakharov, and M. Brown, "Hotter mantle but colder subduction in the Precambrian: What are the implications?" Precambrian Res. **330**, 20–34 (2019).

L. L. Perchuk, A. V. Krotov, T. V. Gerya, "Petrology of the amphibolites of the Tanaelv Belt and granulites of the Lapland Complex," Petrology **7** (4), 339–363 (1999).

L. L. Perchuk, T. V. Gerya, Rinen D. D. Van, and S. A. Smit, "*P-T* Paths and Problems of High-Temperature Polymetamorphism," Petrology **14** (2), 117–153 (2006).

E. S. Persikov and P. G. Bukhtiyarov, "Interrelated structural chemical model to predict and calculate viscosity of magmatic melts and water diffusion in a wide range of composition and T–P parameters of the Earth's crust and upper mantle," Russ. Geol. Geophys. **50** (12), 1079–1090 (2009).

Z. I. Petrova and V. I. Levitskii, *Petrology and Geochemistry of the Granulite Complexes of the Baikal Region* (Nauka, Novosibirsk, 1984) [in Russian].

J. G. Huber M.I. Ramsay, *The Technique of Modern Structural Geology. Volume 2: Folds and Fractures* (Academic Press, London, 1987), pp. 307–700.

N. M. Revyako, Yu. A. Kostitsyn, and Ya. V. Bychkova, "Interaction between a mafic melt and host rocks during formation of the Kivakka layered intrusion, North Karelia," Petrology **20** (2), 101–119 (2012).

K. A. Shurkin, D. P. Vinogradov, F. P. Mitrofanov, and V. M. Shemyakin, *Early Precambrian Magmatic Formations of the USSR. Volume 1. Magmatism of the Early Precambrian* (Nedra, Moscow, 1980) [in Russian].

O. S. Sibilev, M. A. Gogolev, and O. A. Maksimov, "Geological position and conditions of formation of metaenderbites of the Gridino ecologite-bearing mélange zone," Geol. Polezn. Iskop. Karelii. Tr. Karel'sk. Nauchn. Ts. Ross. Akad. Nauk **16**, 5–20 (2013).

S. G. Skublov, A. E. Melnik, Yu. B. Marin, A. V. Berezin, E. S. Bogomolov, and F. I. Ishmurzin, "Geochemistry of zircon rims with different ages in gneisses of the Kola Series (SIMS, SHRIMP-II) and the problem of Early Caledonian thermal activization of the Kola Craton," Dokl. Earth Sci. **453** (3), 1250–1256 (2013).

A. I. Slabunov, *Geology and Geodynamics of Archean Mobile Belts: Evidence from the Belomorian Province of the Fennoscandian Shield* (Izd–vo Karelskogo Nauchnogo tsentra RAN, Petrozavodsk, 2008) [in Russian].

A. I. Slabunov and O. S. Sibilev, "Structure of the Earth's crust of the Belomorian Province of the Fennoscandian shield as reflection of the Early Precambrian geodynamic processes: experience of synthesis of structural-geological, petrological, and geophysical data," *Relation of Surface Structures of the Earth's Crust with Deep-Seated Ones. Proc. 14th International Conference, Petrozavodsk, Russia, 2008* (Izd-vo Karelskogo Nauchnogo tsentra RAN, Petrozavodsk, 2008), Vol. 2, 201–204 [in Russian].

C. André Smit, D. D. van Reenen, C. Roering, R. Boshoff, and L. L. Perchuk, "Neoarchean to Paleoproterozoic evolution of the polymetamorphic Central Zone of the

Limpopo Complex," Geol. Soc. Am. Mem. **207**, 213–244 (2011).

M. M. Stenar and O. I. Volodichev, "On problem of the relict granulite facies of regional metamorphism in the western Belomorian belt," Regional Metamorphism and Metamorphogenic Ore Formation (Nauka, Leningrad, 1970), pp. 137–142 [in Russian].

V. S. Stepanov and A. I. Slabunov, "Amphibolites and carbonate rocks of the Pongoma Bay area (White Sea)," *Precambrian of Northern Karelia* (Izd-vo Karelskogo Nauchnogo tsentra RAN, Petrozavodsk, 1994), pp. 6–30 [in Russian].

N. G. Sudovikov, "Geological overview of the Kuzema–Pongoma area," *International Geological Congress. 17th Session. USSR. Northern Excursion. Karelian ASSR,* Ed. by A. A. Polkanov (Glavnaya redaktsiya geologo-razvedochnoi i geodezicheskoi literatury, Leningrad, 1937), pp. 105–117.

N. G. Sudovikov, *Proceedings on Petrology of the Western Belomorian Belt (Granitization of the Belomorian Rocks)* (GONTI, Leningrad, 1939) [in Russian].

S. S. Sun and W. F. Ms.Donough, "Chemical and isotopic systematises of oceanic basalts: implications for mantle composition and processes," Magmatism in the Ocean Basins, Ed. by A. D. Saunders and M. J. Norry, Geol. Soc. London. Spec. Publ. **42**, 313–346 (1989).

S. A. Svetov, A. V. Stepanova, S. Yu. Chazhengina, E. N. Svetova, A. I. Mikhailova, Z. P. Rybnikova, A. S. Paramonov, V. L. Utitsina, V. S. Kolodei, and M. V. Ekhova, "Precision (ICP-MS, LA-ICP-MS) analysis of composition of rocks and minerals: method and estimation of result accuracy by the example of the Early Precambrian mafic complexes," Geol. Polezn. Iskop. Karelii. Tr. Karel'sk. Nauchn. Ts. RAS, No. 7, 54–73 (2015).

T. Tanaka, S. Togashi, H. Kamioka, et al., "JNdi-1: a neodymium isotopic reference in consistency with LaJolla neodymium," Chem. Geol. **168** (3–4), 279–281 (2000).

O. I. Volodichev, "Early stage metamorphism of the rocks of the Belomorian Complex, Western Baltic Shield," *Geology and Deep Structure* (Leningrad, Nauka, 1975), pp. 43–56 [in Russian]

R. W. White, R. Powell, T. J. B. Holland, et al., "New mineral activity–composition relations for thermodynamic calculations in metapelitic systems," J. Metamorph. Geol. **32** (3), 261–286 (2014).

T. F. Zinger, "Morphological evolution of zircon in polymetamorphic rocks," Dokl. Akad. Nauk **331** (4), 452–455 (1993).

T. F. Zinger, "Morphological evolution of zircon in the Early Precambrian hypersthene diorites of the Pongoma-Navolok massif (Northern Karelia)," Zap. Ross. Mineral. O-va **123** (2), 65–73 (1994).

T. F. Zinger, J. Gotze, O. A. Levchenkov, I. K. Shuleshko, S. Z. Yakovleva, and A. F. Makeyev, "Zircon in polydeformed and metamorphosed precembrian granitoids from the White Sea tectonic Zone, Russia: morphology, cathodoluminiscence, and U-Pb chronology," Int. Geol. Rev. **38** (1), 57–73 (1996).

T. F. Zinger, V. S. Baikova, B. V. Belyatsky, et al. "Morphology and isotopic age of zircons from shear-zones within granitoids of the Belomorian tectonic zone, Baltic Schild, Russia," *Basement Tectonics* (Kluwer Academic Publishers, 1999), Vol. 13, 345–364 (1999).

Translated by E. Kurdyukov